AJNR

Proton Chemical Shift Imaging in Normal Pressure Hydrocephalus

Osamu Kizu, Kei Yamada and Tsunehiko Nishimura

AJNR Am J Neuroradiol 2001, 22 (9) 1659-1664
http://www.ajnr.org/content/22/9/1659

AJNR Am J Neuroradiol 22:1659–1664, October 2001

Proton Chemical Shift Imaging in Normal Pressure Hydrocephalus

Osamu Kizu, Kei Yamada, and Tsunehiko Nishimura

BACKGROUND AND PURPOSE: **Differentiation of normal pressure hydrocephalus (NPH) from other types of dementia and the selection of appropriate candidates for shunt surgery remain a clinical challenge. The aims of this study were to assess the efficacy of cerebral metabolites depicted by proton chemical shift imaging (^{1}H-CSI) in distinguishing NPH from other dementias and to examine the relationship between metabolite changes and the outcome of shunt surgery.**

METHODS: **^{1}H-CSI measurements were obtained in nine patients with clinical diagnosis of NPH; six patients with other types of dementia, including Alzheimer and Pick disease; and five control subjects. The ^{1}H-CSI sequence consisted of a double spin-echo sequence with imaging parameters of 2000/135/4–2 (TR/TE/acquisitions). Volumes of interest were selected from a section through the lateral ventricles. The peak areas and ratios of *N*-acetylaspartate, creatine, choline, and lactate were calculated. In two patients, follow-up ^{1}H-CSI and *N*-isopropyl (^{123}I)-p-iodoamphetamine brain perfusion imaging were available after treatment with continuous spinal drainage.**

RESULTS: **Lactate peaks were observed in the lateral ventricles for all patients with NPH (lactate/creatine, 0.23 ± 0.14) but not for patients with other types of dementia or control subjects. In all cases, we noted no significant differences in the peak ratios in the voxels located at the white matter near the lateral ventricles. In one patient with NPH, intraventricular lactate disappeared and regional CBF recovered after drainage.**

CONCLUSION: **The intraventricular lactate level may be useful in differentiating NPH from other types of dementia.**

Unlike Alzheimer disease or other types of dementia, normal pressure hydrocephalus (NPH) is treatable (1). The diagnosis usually is established on the basis of improved symptoms after shunting of CSF (2, 3). Clinical symptoms of NPH are characterized by mild memory impairment and apathy, ataxic gait, and incontinence (4). Gait deficits commonly are seen in NPH, but mental deterioration may be subtle or even unrecognized. Incontinence appears most often after the appearance of gait disturbance and memory impairment.

Although radioisotope cisternography initially appeared useful in assessing the CSF circulation in NPH (5), several authors have reported that it is unreliable (6). Several studies have measured CBF with single-photon emission CT (SPECT) and xenon CT imaging, and they have revealed reduced CBF in patients with NPH (7–9). Decreased regional cerebral metabolism also has been observed on positron emission tomography (PET) with ^{18}F-2-fluorodeoxyglucose (10, 11). On CT or MR images, patients with NPH may present with symmetrical dilatation of ventricles that is out of proportion to the sulcal enlargement, but these findings are nonspecific. Several reports have described increased velocity of the CSF through the cerebral aqueduct, which can be observed as ''CSF flow void'' on MR imaging (12, 13), but this finding too has been found to be nonspecific (14). Despite these extensive investigations using various neuroimaging studies, many patients with NPH do not present with classic clinical or neuroimaging patterns, and it remains a clinical challenge to distinguish NPH from other types of dementia in many cases.

Furthermore, selection of the appropriate candidates for shunt surgery is difficult. Although CT metrizamide cisternography (15), intracranial pressure measurement (16), and spinal taps (17) are reported to be useful in predicting the response to treatment, the reliability and reproducibility of these tests are limited (18).

Received October 5, 2000; accepted after revision February 9, 2001.

From the Department of Radiology, Kyoto, Japan.

Address reprint requests to Osamu Kizu, MD, Prefectural University of Medicine, 456 Kajiicho, Kamigyoku, Kyoto 602-8566, Japan.

Proton chemical shift imaging (^{1}H-CSI) is a noninvasive method that can depict various metabolites in a wide area of the brain simultaneously. It has been applied to many brain lesions (19–21). Metabolites depicted by ^{1}H-CSI also may aid in understanding the pathophysiology of NPH. The aims of this study were to assess the efficacy of cerebral metabolites detected by ^{1}H-CSI in distinguishing NPH from other dementias and to examine the relationship between metabolite changes and the outcomes of shunt surgery.

Methods

Participants

A total of 20 participants were evaluated with ^{1}H-CSI: nine patients (age range, 49 to 77 years) clinically diagnosed with NPH, six patients with other dementias (four with probable Alzheimer disease, one with Pick disease, and one with frontotemporal dementia; age range, 37 to 67 years), and five healthy age-unmatched control subjects (age range, 24 to 48 years) with no history of psychiatric or neurologic disorders. The diagnosis of NPH was made according to the following criteria: 1) gait disturbance was the first sign of NPH and a predominant symptom; 2) preoperative MR imaging showed severe ventricular dilatation with no cerebral atrophy or diffuse ischemic white matter lesions; 3) there was no identifiable cause for hydrocephalus; 4) there was at least initial improvement of clinical symptoms after continuous spinal drainage, or urinary incontinence and mental deficits (such as memory impairment) were present. The diagnosis of Alzheimer disease was made according to the criteria of the National Institute of Neurological and Communicative Disorders and Stroke-Alzheimer's Disease and Related Disorders Association (22). The diagnoses of Pick disease and frontotemporal dementia were based on the criteria of the International Statistical Classification of Disease and Related Health Problems, 10th revision, and the criteria for frontotemporal dementia proposed by the Lund and Manchester group (23).

MR Examinations

All patients were examined with a 1.5-T whole-body MR imaging system (Magnetom H15 SP; Siemens, Erlangen, Germany) operating at 63.67 MHz for ^{1}H-CSI, using the conventional cross-paralleled head coil.

From the transverse and sagittal T1-weighted spin-echo brain imaging with parameters of 200/15 (TR/TE), an 8-mm section thickness, and 2-mm intersection gap, we selected a volume of interest (VOI) 15 mm thick from periventricular regions. The anteroposterior and left-to-right dimensions of the VOI (102–90 × 92–80 mm) were adjusted for each subject according to brain size. This rectangular VOI was selected to exclude contamination of signal from the skull and subcutaneous fat.

The magnet was shimmed on the ^{1}H water signal of the localized VOI to a line width of about 8 Hz (full width at half-maximum). The ^{1}H-CSI sequence consisted of a double spin-echo sequence with parameters of 2000/135/4–2 (TR/TE/acquisitions). Before data acquisition, we applied a chemical shift-selective pulse with a dephasing gradient for water suppression. We applied two-directional, 16 × 16 phase-encoding steps over a field of view (160 × 160 or 180 × 180 mm) at the level of the periventricular white matter. This resulted in a nominal in-plane resolution of 10–11 mm, and a nominal ^{1}H-CSI voxel size of 1.5–1.9 mL before zero-filling. We measured the ^{1}H-CSI data without water suppression to correct for eddy-current distortions. The entire examination took about 60 minutes.

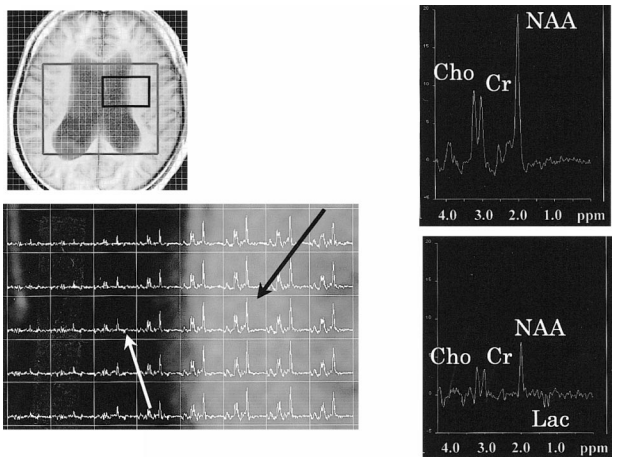

FIG 1. Proton MR spectra (TR/TE, 2000/135) in the patient with NPH. Upper left, axial T1-weighted MR image of the same patient. A box outlines volume of interest, which includes the bodies of lateral ventricles in the hemisphere. Lower left corner shows spectra from the body of the left lateral ventricle and surrounding parenchyma. The spectrum from the voxel of the parenchyma (*black arrow*) shows normal spectral pattern (upper right). The spectrum from the voxel in the body of left lateral ventricle (*white arrow*) shows the lactate peak (lower right). NAA, Cho, and Cr peaks also are observed, suggesting that this intraventricular voxel contains periventricular brain tissue.

The ^{1}H-CSI data sets were processed with custom spectroscopic imaging software on a SPARC station 20 workstation (Sun Microsystems, Mountain View, CA). The spatial dimensions were zero-filled to 32 points, and the time dimension was filtered with a gaussian filter. After a 2D Fourier transformation, we corrected the baseline by subtracting the fitted five-dimensional polynomial curve. The phase was adjusted by an *N*-acetylaspartate (NAA) peak by using a linear or constant-phase angle.

The three major resonances in the spectra (NAA, choline [Cho], creatine [Cr]) and lactate were curve-fitted, and peak areas were obtained from all voxels. When we selected the voxels from the periventricular region, T1-weighted MR imaging was used to exclude CSF space. Peak areas of NAA, Cho, and Cr were used to calculate metabolite signal ratios. We positively identified the lactate peaks only when they were inverted doublet peaks at 1.3 ppm, with the peak level 1.5 times higher than the noise level, and only when similar peaks were observed in the surrounding voxels. Lactate was estimated by the lactate:Cr ratio, using Cr from the periventricular voxels, which is relatively stable in adults. We verified the calculation of periventricular peak-area without volume collection against MR images, which revealed that the chosen voxels contained no CSF space.

Statistical Analysis

The metabolite ratios were summarized as means ± SD. One-way analysis of variance was applied to test for significant differences in the metabolite ratios. Statistical significance was set at $P < .05$.

In two patients, a follow-up ^{1}H-CSI was available after continuous spinal drainage. In a single case, the data also were compared with those from ^{123}I iodoamphetamine brain perfusion SPECT imaging.

Results

Lactate peaks were observed in the lateral ventricles for all patients with NPH (lactate:Cr, 0.23 ±

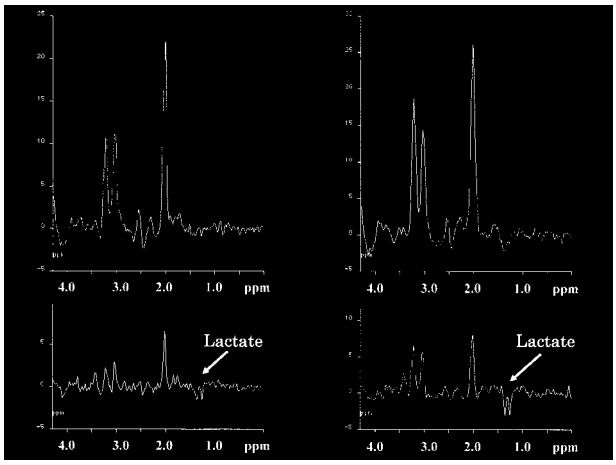

FIG 2. Proton MR spectra (TR/TE, 2000/135) in two patients with NPH. The spectra obtained from periventricular regions (upper row) with the intraventricular spectra (lower row) are shown. Apparent inverted doublet peaks at 1.3 ppm are observed in the intraventricular spectrum of one case (left side) and can be recognized as lactate peaks. In the other case (right side), good qualities of lactate peaks are seen compared with the peaks from the periventricular region in the upper row.

0.14 [Figs 1 and 2]) but not in the control subjects or patients with other dementias (Table). Peaks for NAA, Cho, and Cr were found in the voxels of the ventricles, which suggested partial volume artifact from periventricular brain tissue.

In the voxels from periventricular regions, there was no lactate peak or significant difference in peak ratios among these cases (Fig 2, Table); for NAA:Cho, the values were 2.13 ± 0.43 for patients with NPH, 2.03 ± 0.47 for patients with other dementias, and 2.18±0.44 for control subjects (P = .851); for NAA:Cr, they were 1.63 ± 0.19, 1.54 ± 0.23, and 1.51 ± 0.39, respectively (P = .694), and for Cho:Cr, they were 0.78 ± 0.10, 0.79 ± 0.17, and 0.74 ± 0.26, respectively (P = .86).

Intraventricular lactate peaks had disappeared in one patient (lactate:Cr decreased from 0.21 to 0.00), and regional CBF had recovered to normal on spectra after continuous spinal drainage (Fig 3). The patient's moderate memory loss before the procedure (Mini-Mental Scale Examination score, 23/30) was not improved significantly after treatment. Gait disturbance and incontinence became worse.

In the other patient with a follow-up study, intraventricular lactate peaks were slightly increased after continuous spinal drainage. The lactate:Cr ratio had changed from 0.18 to 0.21. After treatment, there was no change in symptoms such as gait disturbance or incontinence. There had been only limited symptoms of dementia, and they also did not change.

Discussion

The most striking point elucidated in this study was the intraventricular lactate peaks, observed only in the patients with NPH, not in the patients with other dementias or in the control subjects. Although clinical symptoms continue to play the main

Peak ratios in patients with NPH, patients with other dementias, and control subjects

	Periventricular White Matter			Lactate/Cr in Lateral Ventricles	
	NAA/Cho	NAA/Cr	Cho/Cr	Before*	After**
NPH					
Case 1	2.11	1.66	0.79	0.15	· · ·
Case 2	1.46	1.28	0.88	0.18	0.21
Case 3	2.26	1.55	0.69	0.10	· · ·
Case 4	1.75	1.62	0.93	0.55	· · ·
Case 5	2.50	1.94	0.78	0.21	(—)
Case 6	2.36	1.63	0.69	0.12	· · ·
Case 7	1.61	1.47	0.91	0.21	· · ·
Case 8	2.70	1.76	0.65	0.25	· · ·
Case 9	2.39	1.75	0.73	0.30	· · ·
Other dementias					
Alzheimer disease, Case 1	2.88	1.61	0.56	(—)	· · ·
Alzheimer disease, Case 2	2.05	1.30	0.64	(—)	· · ·
Alzheimer disease, Case 3	2.02	1.47	0.73	(—)	· · ·
Alzheimer disease, Case 4	1.90	1.83	0.97	(—)	· · ·
Pick disease	1.88	1.77	0.94	(—)	· · ·
Frontotemporal dementia	1.45	1.27	0.87	(—)	· · ·
Control subjects					
Case 1	2.04	1.49	0.73	(—)	· · ·
Case 2	2.94	0.87	0.29	(—)	· · ·
Case 3	2.02	1.67	0.83	(—)	· · ·
Case 4	1.78	1.63	0.92	(—)	· · ·
Case 5	2.11	1.91	0.91	(—)	· · ·

* Before continuous spinal drainage.
** After continuous spinal drainage.

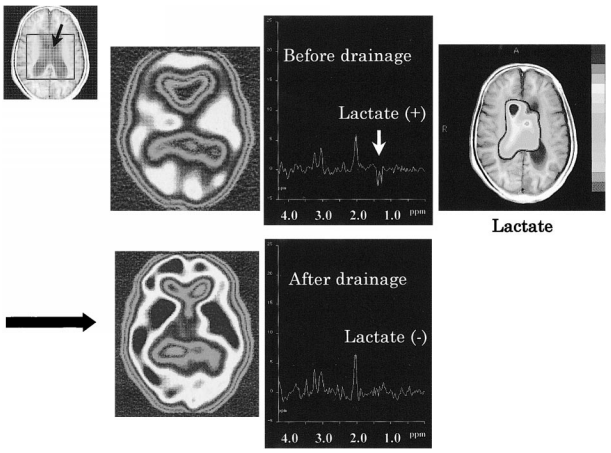

FIG 3. Proton MR spectra (TR/TE, 2000/135) before and after continuous spinal drainage in the lateral ventricle of a patient with NPH. The spectra were obtained from a intraventricular voxel (*black arrow in VOI*). Before treatment, lactate peaks are observed as inverted doublet peaks at 1.3 ppm from the intraventricular voxel of NPH (upper middle). Cho, Cr, and NAA peaks suggest partial volume artifact from periventricular brain tissue. A metabolic image of lactate (upper right) before treatment shows that lactate is confined to the lateral ventricles and surroundings. After treatment, lactate is not observed clearly (lower right). The reduced CBF (upper left) returned to normal after continuous spinal drainage (lower left) at SPECT.

role in diagnosing various types of dementia, it is sometimes difficult to diagnose NPH by clinical symptoms alone. Gait impairment remains the characteristic symptom of NPH, but dementia and incontinence may not be recognized. This classic clinical triad may not be displayed at the same time. Diagnostic imaging studies, such as CT and MR imaging, also are helpful in differentiating dementias. Dilatation of the temporal horns of the lateral ventricles is one of the characteristics of NPH (24), but this also is observed in patients with Alzheimer disease. There is a report that the degree of dilatation of perihippocampal fissures is a useful marker for differentiating Alzheimer disease from NPH (25). Findings such as dilated sulci and ventricles by CT and MR imaging are observed in most patients with dementia, however, and they are nonspecific. Reduced focal CBF and metabolic activity observed by SPECT and PET are not pathognomonic for dementia. In these situations, the lactate observed by ^{1}H-CSI helps differentiate NPH from other types of dementia.

Hakim and Adams first described NPH (2, 26) as symptomatic hydrocephalus with normal cerebrospinal pressure. Hakim et al (26) hypothesized that the pathophysiology of NPH that increased intraventricular pressure caused dilatation of the ventricle with stretching of the periventricular parenchyma, which resulted in normalization of the intraventricular pressure. Experiments in chronic, communicating hydrocephalus in dogs have shown that intraventricular CSF pressure increases at first but later falls into the normal range after dilatation of the ventricles (27). During the initial stage, intraventricular pressure may be elevated in NPH, and this may cause periventricular ischemia with arterial compression. On the other hand, continuous recordings of intraventricular CSF pressure in hydrocephalic patients have revealed that the episodic CSF pressure elevations mainly consist of so-called B-waves (28). Elevation of intraventricular pressure during sleep also has been reported (29). These reports suggest slight elevations in intraventricular CSF pressure and do not conflict with the feasibility of periventricular ischemia.

Lactate is the end-product of nonoxidative metabolism and suggests the presence of ischemic changes. Lactate also is produced by increased glycolysis in tumors and inhibition of pyruvate dehydrogenase, one of the enzymes in the tricarboxylic-acid cycle. There have been some reports concerning lactate in experimental hydrocephalus observed by MR spectroscopy (MRS) (30–32). In these reports, proton MRS of a CSF phantom with a normal lactate concentration revealed no lactate peak, indicating that the in vivo detection of lactate reflects elevated CSF lactate peaks. This could not be explained by a prolonged T2 in CSF at normal concentrations. It was assumed that, if anaerobic conditions were restricted to periventricular brain tissue, the elevated lactate in CSF could easily be explained by regional lactate production, in view of the proton MRS voxel localization. In hydrocephalus, ventricular enlargement has been reported to cause displacement of primary cerebral arteries and reductions in the number and caliber of the microvessels, resulting in diminished CBF and cerebral edema (33). The precise reason for the presence of intraventricular lactate is unclear. It is conceivable that the lactate reflects ischemic changes in the periventricular regions. In the patients with NPH, the relative stasis of the CSF in the lateral ventricles may have resulted in elevated lactate. There were no intraventricular lactate peaks in the control subjects or the patients with other types of dementia. Because the distortion of the baseline and the peak-to-peak noise in their spectra were as same as those in patients with NPH, we considered that we were able to observe lactate in the patients with NPH because their lactate levels were higher than those in the other groups.

There was no reduction in NAA concentration in the cerebral parenchyma of patients with NPH. The presence of intraventricular lactate suggests ischemic changes in the brain tissue, which usually are associated with reduced NAA concentrations. It seems paradoxical that there was a normal level of NAA with detectable levels of intraventricular lactate. Normal NAA concentrations have been reported in hydrocephalus in infants (34); the authors stated that the reduction in CBF might be insufficient to result in metabolic changes detectable by ^{1}H-CSI.

The spectral patterns in the periventricular regions also were normal in patients with other types

of dementias, such as probable Alzheimer disease, Pick disease, and frontotemporal dementia. Some reports, however, have described reduced NAA concentrations in the occipital cortex and hippocampi in patients with Alzheimer disease (35–37). Patients with Alzheimer disease show general cortical atrophy and reductions in gray matter with disproportionate loss of volume in the temporal lobes and hippocampi. In Pick disease and frontotemporal dementia, cortical atrophy also is one of the pathologic characteristics, but there may be less metabolic change near lateral ventricles. One reason for normal periventricular NAA levels in these patients with dementia is that their NAA was measured from the periventricular voxels, which contained small amounts of gray matter or cortical regions.

Intraventricular lactate can be used to differentiate NPH from other types of dementia. ^{1}H-CSI is especially important when NPH cannot be diagnosed by clinical symptoms, morphologic imaging, such as CT or MR imaging, and functional imaging studies, such as PET. ^{1}H-CSI also may be useful as a follow-up study after continuous spinal drainage; in one of our patients, the intraventricular lactate peaks observed before treatment had disappeared after drainage.

Conclusion

Intraventricular lactate in NPH may be a key factor in differentiating NPH from other dementias. This metabolite reflects ischemic changes in the periventricular regions despite normal CSF pressures in patients with NPH.

References

1. Mahler CE, Cummings JL, Benson DF. **Treatable dementia.** *West J Med* 1987;146:700–712
2. Adams RD, Fisher CM, Hakim S, et al. **Symptomatic occult hydrocephalus with "normal" cerebrospinal fluid pressure.** *N Engl J Med* 1965;273:117–126
3. Ojemann RG. **Normal pressure hydrocephalus.** *Clin Neurosurg* 1970;18:337–370
4. Masters JC, O'Grady M. **Normal pressure hydrocephalus. A potentially reversible form of dementia.** *J Psychosoc Nurs Ment Health Serv* 1992;30:25–28
5. Benson DF, LeMay M, Patten DH, Rubens AB. **Diagnosis of normal-pressure hydrocephalus.** *N Engl J Med* 1970;283:609–615
6. Vanneste J, Augustijn P, Davies GA, Dirven C, Tan WF. **Normal-pressure hydrocephalus. Is cisternography still useful in selecting patients for a shunt?** *Arch Neurol* 1992;49:366–370
7. Graff-Radford NR, Rezai K, Godersky JC, Eslinger P, Damasio H, Kirchner PT. **Regional cerebral blood flow in normal pressure hydrocephalus.** *J Neurol Neurosurg Psychiatry* 1987;50: 1589–1596
8. Larsson A, Bergh AC, Bilting M, et al. **Regional cerebral blood flow in normal pressure hydrocephalus: diagnostic and prognostic aspects.** *Eur J Nucl Med* 1994;21:118–123
9. Nakano H, Bandoh K, Miyaoka M, Sato K. **Evaluation of hydrocephalic periventricular radiolucency by dynamic computed tomography and xenon-computed tomography.** *Neurosurgery* 1996;39:758–762
10. Jagust WJ, Friedland RP, Budinger TF. **Positron emission tomography with [18F]fluorodeoxyglucose differentiates normal pressure hydrocephalus from Alzheimer-type dementia.** *J Neurol Neurosurg Psychiatry* 1985;48:1091–1096
11. Tedeschi E, Hasselbalch SG, Waldemar G, et al. **Heterogeneous cerebral glucose metabolism in normal pressure hydrocephalus.** *J Neurol Neurosurg Psychiatry* 1995;59:608–615
12. Bradley WG Jr, Whittemore AR, Watanabe AS, Davis SJ, Teresi LM, Homyak M. **Association of deep white matter infarction with chronic communicating hydrocephalus: implications regarding the possible origin of normal-pressure hydrocephalus.** *Am J Neuroradiol* 1991;12:31–39
13. Schroth G, Klose U. **Cerebrospinal fluid flow. II. Physiology of respiration-related pulsations.** *Neuroradiology* 1992;35:10–15
14. Krauss JK, Regel JP, Vach W, Jungling FD, Droste DW, Wakhloo AK. **Flow void of cerebrospinal fluid in idiopathic normal pressure hydrocephalus of the elderly: can it predict outcome after shunting?** *Neurosurgery* 1997;40:67–73
15. Huckman MS. **Normal pressure hydrocephalus: evaluation of diagnostic and prognostic tests.** *Am J Neuroradiol* 1981;2: 385–395
16. Black PM, Ojemann RG, Tzouras A. **CSF shunts for dementia, incontinence, and gait disturbance.** *Clin Neurosurg* 1985;32: 632–651
17. Wikkelso C, Andersson H, Blomstrand C, Lindqvist G. **The clinical effect of lumbar puncture in normal pressure hydrocephalus.** *J Neurol Neurosurg Psychiatry* 1982;45:64–69
18. Vanneste JA. **Diagnosis and management of normal-pressure hydrocephalus.** *J Neurol* 2000;247:5–14
19. Luyten PR, Marien JH, Heindel W, et al. **Metabolic imaging of patients with intracranial tumors: H-1 MR spectroscopic imaging and PET.** *Radiology* 1990;176:791–799
20. Fulham HJ, Bizzi A, Dietz MJ, et al. **Mapping of brain tumor metabolites with proton MR spectroscopic imaging: clinical relevance.** *Radiology* 1992;185:675–686
21. Constans JM, Meyerhoff DJ, Gerson J, et al. **H-1 MR spectroscopic imaging of white matter signal hyperintensities: Alzheimer disease and ischemic vascular dementia.** *Radiology* 1995;197:517–523
22. McKhann G, Drachman D, Folstein M, Katzman R, Price D, Stadlan EM. **Clinical diagnosis of Alzheimer's disease: report of the NINCDS-ADRDA Work Group under the auspices of Department of Health and Human Services Task Force on Alzheimer's Disease.** *Neurology* 1984;34:939–944
23. The Lund and Manchester Groups. **Clinical and neuropathological criteria for frontotemporal dementia.** *J Neurol Neurosurg Psychiatry* 1994;57:416–418
24. George AE, Holodny A, Golomb J, de Leon MJ. **The differential diagnosis of Alzheimer's disease. Cerebral atrophy versus normal pressure hydrocephalus.** *Neuroimaging Clin N Am* 1995;5: 19–31
25. Holodny AI, Waxman R, George AE, Rusinek H, Kalnin AJ, de Leon M. **MR differential diagnosis of normal-pressure hydrocephalus and Alzheimer disease: significance of perihippocampal fissures.** *Am J Neuroradiol* 1998;19:813–819
26. Hakim S, Adams RD. **The special clinical problem of symptomatic hydrocephalus with normal cerebrospinal fluid pressure. Observations on cerebrospinal fluid hydrodynamics.** *J Neurol Sci* 1965;2:307–327
27. James AE Jr, Burns B, Flor WF, et al. **Pathophysiology of chronic communicating hydrocephalus in dogs (*Canis familiaris*). Experimental studies.** *J Neurol Sci* 1975;24:151–178
28. Symon L, Dorsch NW. **Use of long-term intracranial pressure measurement to assess hydrocephalic patients prior to shunt surgery.** *J Neurosurg* 1975;42:258–273
29. Di Rocco C, McLone DG, Shimoji T, Raimondi AJ. **Continuous intraventricular cerebrospinal fluid pressure recording in hydrocephalic children during wakefulness and sleep.** *J Neurosurg* 1975;42:683–689
30. Braun KP, de Graaf RA, Vandertop WP, Gooskens RH, Tulleken KA, Nicolay K. **In vivo 1H MR spectroscopic imaging and diffusion weighted MRI in experimental hydrocephalus.** *Magn Reson Med* 1998;40:832–839
31. Braun KP, van Eijsden P, Vandertop WP, et al. **Cerebral metabolism in experimental hydrocephalus: an in vivo 1H and 31P magnetic resonance spectroscopy study.** *J Neurosurg* 1999;91: 660–668
32. Braun KP, Dijkhuizen RM, de Graaf RA, et al. **Cerebral ischemia and white matter edema in experimental hydrocephalus: a combined in vivo MRI and MRS study.** *Brain Res* 1997;757: 295–298
33. Wozniak M, McLone DG, Raimondi AJ. **Micro- and macrovascular changes as the direct cause of parenchymal destruction**

in congenital murine hydrocephalus. *J Neurosurg* 1975;43: 535–545
34. Bluml S, McComb JG, Ross BD. **Differentiation between cortical atrophy and hydrocephalus using 1H MRS.** *Magn Reson Med* 1997;37:395–403
35. Shonk TK, Moats RA, Gifford P, et al. **Probable Alzheimer disease: diagnosis with proton MR spectroscopy.** *Radiology* 1995; 195:65–72
36. Adalsteinsson E, Sullivan EV, Kleinhans N, Spielman DM, Pfefferbaum A. **Longitudinal decline of the neuronal marker *N*-acetyl aspartate in Alzheimer's disease.** *Lancet* 2000;355: 1696–1697
37. Schuff N, Amend D, Ezekiel F, et al. **Changes of hippocampal *N*-acetyl aspartate and volume in Alzheimer's disease. A proton MR spectroscopic imaging and MRI study.** *Neurology* 1997;49:1513–1521